Amyloid-like protein nanofibrous membranes as a sensing layer infrastructure for the design of mass-sensitive biosensors

Gözde Kabay, Gizem kaleli Can, Mehmet Mutlu

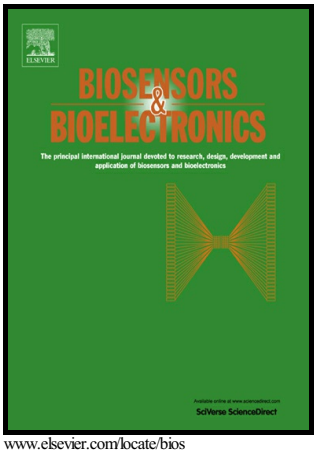

www.elsevier.com/locate/bios

PII: S0956-5663(17)30393-7
DOI: http://dx.doi.org/10.1016/j.bios.2017.06.016
Reference: BIOS9786

To appear in: *Biosensors and Bioelectronic*

Received date: 21 March 2017
Revised date: 1 June 2017
Accepted date: 8 June 2017

Cite this article as: Gözde Kabay, Gizem kaleli Can and Mehmet Mutlu Amyloid-like protein nanofibrous membranes as a sensing layer infrastructure fo the design of mass-sensitive biosensors, *Biosensors and Bioelectronic* http://dx.doi.org/10.1016/j.bios.2017.06.016

Amyloid-like protein nanofibrous membranes as a sensing layer infrastructure for the design of mass-sensitive biosensors

Gözde KABAY[a], Gizem KALELİ CAN[a], Mehmet MUTLU[a,b,*]

[a]Plasma Aided Biomedical Research Group (pabmed), Biomedical Engineering Division, Graduate School of Science and Technology, TOBB University of Economics and Technology, Ankara 06560, Turkey

[b]Plasma Aided Biomedical Research Group (pabmed), Department of Biomedical Engineering, TOBB University of Economics and Technology, Ankara 06560, Turkey

[*]Corresponding author: Mehmet MUTLU. Söğütözü Caddesi No: 43, Söğütözü, Ankara 06560, Turkey. Tel.: +90 (312) 492 42 68, Fax: +90 (312) 287 19 46, Email: m.mutlu@etu.edu.tr

Abstract

Quartz crystal microbalances (QCMs) have been used in the literature for mass sensitive biosensor applications. However, their performance, reliability and stability have been limited by the chemical treatment steps required for the functionalization and activation of the QCM surface, prior to antibody immobilization. Specifically, these steps cause increased film thickness, which diminishes performance by mass overload, and create a harsh environment, which reduces biological activity. In this work, we eliminated this chemical step by introducing a sensing layer modification using electrospun amyloid like-bovine serum albumin (AL-BSA) nanofibers on QCM surfaces. Owing to the self-functionality of AL-BSA nanofibers, these modified QCM surfaces were directly activated by glutaraldehyde (GA). To assess the performance of these modified electrodes, a model protein, lysozyme (Lys), was selected as the biological agent to be immobilized. Frequency measurements were performed in batch (dip-and-dry) and continuous (flow-cell) processes, and binding performances were compared.

AL-BSA modified surfaces were characterized by X-ray photoelectron spectroscopy (XPS), scanning electron microscope (SEM), quartz crystal microbalance (QCM), contact angle (CA) and attenuated total reflectance-Fourier transform infrared spectroscopy (ATR-FTIR). Protein detection was measured based on the frequency shift before and after the covalent bonding of Lys. Under optimized conditions, the proposed immobilization platforms could bind 335 ng/mL and 250 ng/mL of Lys for batch and continuous processes, respectively. Our results demonstrate the potential usage of these self-functional electrospun AL-BSA infrastructure sensing layers on QCM surfaces. This modification enables the direct immobilization of bioactive agents by eliminating any surface functionalization process for further mass-sensitive biosensor applications.

Keywords: Amyloid-like protein; Bovine serum albumin; Lysozyme; Electrospinning; Quartz crystal microbalance; Protein immobilization.

1. Introduction

Mass-sensitive biosensors for biomedical applications represent a major challenge in nanotechnology. A quartz crystal microbalance (QCM) is a frequently used acoustic wave mass-sensitive detector. QCMs are extremely sensitive to mass (density) and to viscoelastic changes at the solid-solution interface, and can respond to any changes in mass at this interface with a resolution of 1 ng/cm^2. When a foreign mass is attached on the surface of the QCM, it affects the resonant frequency of the oscillating crystal. The oscillations become stable only when the natural resonance frequency is achieved (Bard et al., 2008; Ferreira et al., 2009; Lu and Czanderna, 2012; O'sullivan and Guilbault, 1999). Subsequently, the change in the natural resonance frequency becomes proportional to the mass deposited on the QCM electrode. This can be directly calculated using the Sauerbrey equation (Sauerbrey, 1959).

The modification of the QCM surface through the creation of a recognition layer is crucial in achieving highly sensitive and selective mass-sensitive biosensors for biomolecule detection. Biofunctionalized thin films may be adsorbed on the surface of the QCM crystal with the added possibility of tuning the polymer composition to ensure that the binding is completely achieved. Various polymeric layers, including cellulose acetate, polyurethane, polystyrene, polyethylene amine, polybutyl methacrylate, polyvinyl formal/ethylal, polyvinylalcohol, and polyethyleneimine have been used for the preparation of sensing layers for mass-sensitive sensors (Alp et al., 2000; Jenik et al., 2009; Koshets et al., 2003; Öztürk et al., 2008; Rodoplu et al., 2013; Tsai et al., 2011; Zhang et al., 2003). Additionally, various coating methods including silanization, immobilization on the pre-coated crystal, entrapment, or cross-linking methods are used for antibody binding onto the quartz crystal (Jenik et al., 2009; Mutlu, S., 2011; Öztürk et al., 2008; Park and Kim, 1998; Park et al., 2003; Park et al., 2004; Rodoplu et al., 2013; Tsai et al., 2011). In addition to these techniques, plasma polymerization systems have proven useful for the modification of the surface of the quartz crystal (Karamollaoğlu et al., 2009; Mutlu et al., 1999; Mutlu et al., 2008; Nakanishi et al., 1996; Wu et al., 2000) to enhance QCM sensitivity, and for improving the immobilization capacity of bioactive agents, through the creation of functional groups on recognition layers (Akdoğan et al., 2006; Mutlu et al., 2008). Although improvements have been achieved with these techniques, the interactions of bioactive agents within the QCM electrode surface area were limited and resulted in low signal transduction. Moreover, the final film could be too thick, and diminish the performance of the quartz crystal. Film stability also represents an important issue in the preparation of mass-sensitive biosensors using quartz crystals. To overcome all of these problems, including the limited surface area, our research group as well as others have considered nanoscale approaches (Ayad et al., 2014; Dincel and Mutlu, 2015; Rodoplu et al., 2013; Xu et al., 2016). However, surface functionalization of sensing layers, as a multistep process for achieving the successful immobilization of bioactive agents, remains challenging.

Electrospinning represents one of the easiest material-processing methods, which is suitable for nanoscale surface modification of several kinds of materials, including piezoelectric transducers. The larger surface-area-to-volume ratio of electrospun membranes results in a higher immobilization of biological agents, as compared to that observed using flat films or microfibers (Ayad et al., 2014; Dincel and Mutlu 2015; Kabay et al., 2016; Rodoplu et al., 2013; Xu et al., 2016). However, the chemical composition of most synthetic polymers is unsuitable for direct antibody immobilization. Thus, additional chemical modifications are required to create functional groups that assist in the binding of bioactive agents. For the elimination of this chemical step, protein structures may be preferred instead of synthetic

polymers (Kabay et al., 2016; Khadka and Haynie, 2012; Nuansing et al., 2013), as the amine groups present in proteins can be directly activated prior to immobilization. Additionally, proteins which exist in an amyloid-like form exhibit high mechanical strength and film stability during processing (Cinar et al., 2012; Dror et al., 2008; Kowalczyk et al., 2008; Raynes and Gerrard 2013). Further, proteins in nanofibers which are present in an amyloid-like form represent a completely natural material, and show great potential for use in any type of medical, pharmaceutical, or life-science applications.

So far, no reports have been published on the modification of the amyloid-like nanofibers on QCM gold electrode surfaces. In this study, a three-dimensional (3D) protein-capturing surface was fabricated using AL protein nanofibers, to develop a fully natural infrastructure for a biosensor. The modification was performed through the electrospinning of an AL-BSA solution over QCM surfaces. Lysozyme (Lys) was selected as a model protein to be immobilized, and modified membranes were directly activated by glutaraldehyde prior to frequency measurements, to evaluate performance parameters, such as sensitivity, repeatability, and protein immobilization capacity.

2. Materials and methods

2.1. Materials

Glucose oxidase (GOD) from *Aspergillus niger* (SA: 306 U/mg), 2,2,2-trifluoroethanol (TFE), β-mercaptoethanol (β-ME), glutaraldehyde (GA), ultra-pure water (PW), sulphuric acid (H_2SO_4), and hydrogen peroxide (H_2O_2) were purchased from Sigma-Aldrich (St. Louis, MO, USA). All other reagents, including sodium chloride (NaCl), disodium hydrogen phosphate (Na_2HPO_4), and sodium dihydrogen phosphate (NaH_2PO_4), which were used as buffering agents, lysozyme (Lys) and bovine serum albumin (BSA) were supplied by Acros Organics (Morris Plains, NJ, USA). Double-distilled water was used in all experiments.

2.2. Fabrication of amyloid-like membrane modified QCM electrodes

For the preparation of AL-BSA modified QCM crystals (ES-QCM), we used AT-cut quartz crystals with gold electrodes, having a frontal electrode diameter of 12.8 mm with a fundamental frequency of 5 MHz (Maxtek Inc.; Santa Fe Springs, CA, USA). Before the quartz crystals were used, a piranha solution was prepared using a 1:3 mixture of 30 % (v/v) H_2O_2 and H_2SO_4. The cleaning procedure for gold electrodes was performed as previously described (Kern, 1993). Gold electrodes were washed in double-distilled water and ethanol before use, and dried at 25 °C. Blank QCM (B-QCM) frequency values were recorded to evaluate the frequency shift caused by the harsh cleaning process.
For the electrospinning solution, BSA was dissolved in a mixture of TFE and phosphate-buffered saline (PBS) to obtain a 12 % (w/v) final solution at 25 °C. The tertiary structure of the protein was decomposed using β-ME, and stabilized by the addition of TFE, as reported elsewhere (Kabay et al., 2016). The BSA containing solvent was stirred continuously at 25 °C for 4 h. Prior to the modification process, the QCM was placed over an aluminium collector with a homemade cap containing a hole in the centre, and the gold electrode was exposed to nanofiber formation. For the electrospinning setup, a direct current (DC) voltage supplier (MCH 303D2; Gamma High Voltage Research Inc., Ormond Beach, FL, USA) and a syringe pump (NE-1000; New Era Pump Systems Inc., Farmingdale, NY, USA) were used.
A vertically fixed 5-mL syringe with a metal needle (inner diameter: 0.80 mm) was filled with the AL-BSA solution. In the vertical setup, the collector was placed on the floor and the syringe pump was located above the collector. In our preliminary studies, the flow rates were

maintained between 0.20 and 0.40 mL/h (Fig. 1), the applied voltage and the distance between the tip and collector was varied from 12–20 kV and 8–15 cm, respectively. All experiments were performed at atmospheric pressure and at room temperature (~25 °C). All samples were placed in a vacuum desiccator for drying, and stored in the desiccator overnight at room temperature before the initial frequency values for B-QCMs and ES-QCM were recorded in the gaseous phase.

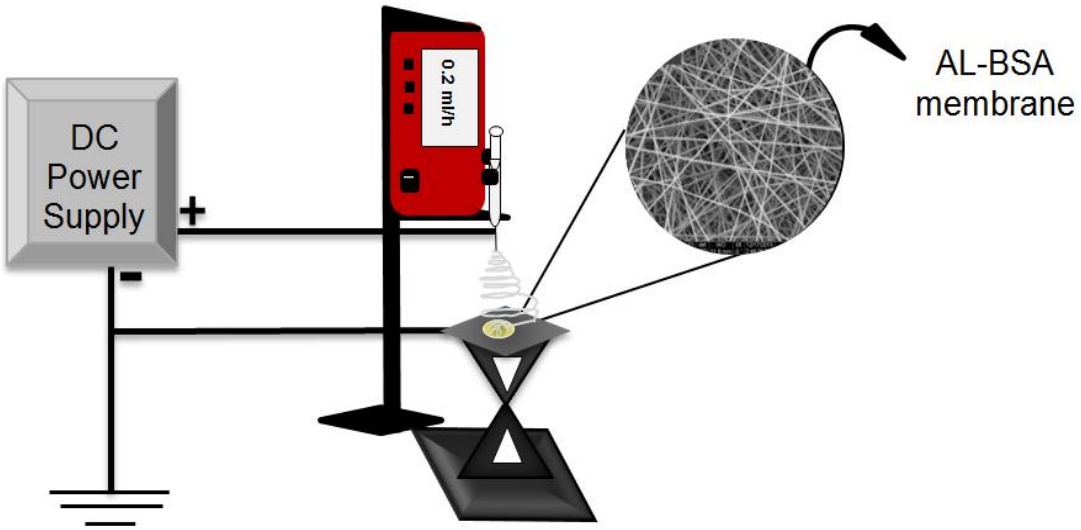

Fig. 1. A schematic diagram illustrating the electrospinning deposition of amyloid-like BSA nanofibres on QCM gold electrode surface.

Finally, QCM surfaces were modified using three different fibre collection times: 30, 60, and 120 s, to investigate the immobilization capacity for the bioactive agent (Lys), as a function of the accumulated amount of functional nanofibers.

2.3. Glutaraldehyde activation

In the case of the GA modification, we tried to minimize the destruction of nanofibers during the activation process to increase the surface area to volume ratio at the nanoscale level, and to achieve an appropriate level of active group formation on the surface. For surface activation, all ES-QCMs were immersed in a 2.5 % (v/v) GA solution and placed in a shaker to be stirred (300 rpm) at room temperature for 1–24 h. After the activation process, all QCMs were washed three times with phosphate buffer (pH 7.4) and double-distilled water. As a negative control (NC), 2 h GA modified B-QCMs were prepared to investigate the effect of nanofiber modifications on the sensitivity and frequency shift.

2.4. Physical and chemical characterization of AL-BSA modified gold electrodes

The effects of the processing parameters and that of the GA activation period on the morphology of the nanofiber were evaluated by scanning electron microscopy (SEM, FEI-Quanta 200; Hillsboro, OR, USA). The samples were sputter-coated with gold, prior to microscopic examination. The average fibre diameter in the samples was determined by measuring the diameters obtained from the SEM images using the ImageJ software, and the graphs were the analysed using the OriginLab Software v.6 (Wellesley Hills, MA, USA).

The static contact angles of the electrode surfaces, before and after the modification of the nanofiber and the activation of GA, were measured in five samples for each modified group. To examine contact angle differences due to electrode modification, a sessile water drop was placed on the electrode surface. The volume of the water drop deposited on the membrane surface was 20 µL. The contact angle (CA) values were calculated using the ImageJ software (NIH, MD, USA).

The chemical groups on the ES-QCM and ES/GA-QCM surfaces and the pure GA were characterized using attenuated total reflectance-Fourier transform infrared spectroscopy (ATR-FTIR) (Perkin Elmer Spectrum, Waltham, MH, USA). ATR-FTIR spectra were measured across a wavenumber range of 4000–1000 cm^{-1}.

The surface composition of the samples was characterized by X-ray photoelectron spectroscopy (XPS). The XPS characterization of the materials was done using a Thermo K-Alpha (Thermo Fisher Sci., Waltham, MA, USA) instrument and performed with a Thermo K-Alpha monochromatic high-performance XPS spectrometer (Thermo Fisher Sci., Waltham, MA, USA) at a pressure of 1×10^{-9} Torr. The ultrahigh resolution energy and the survey pass energy were adjusted to 30 eV and 200 eV, respectively. The spot size was 400 µm per sample. For quantification, the relative sensitivity factors given by the XPS instrument supplier were used. The fitting of the XPS spectra was performed using the OriginLab Software v.6, and is presented in the Supplementary materials.

2.5. Protein immobilization over QCM surfaces and frequency measurements

The bioactive agent (Lys) immobilization capacity of the nanofibers depends on the collection period during which it was studied. For this purpose, glutaraldehyde activated B-QCMs and ES/GA-QCMs, which were produced under the 30, 60, and 120 s fibre collection times, were used for the frequency measurement.

In the dip-and-dry process, the ES/GA-QCMs and the B-QCMs were treated with a 200 ng/mL (w/v) Lys (0.1 % v/v in PBS, pH 7.4) solution for 2 h, cleaned with PBS and distilled water to remove unbounded Lys from the modified QCM surface, and air-dried.

In the second step, a continuous process was employed for the quantification of Lys immobilization over ES/GA-QCMs and B-QCM surfaces. Experiments were started with the introduction of PBS into the flow medium, and then the steady state baseline resonant frequencies of the ES/GA-QCMs were determined. Solutions containing biological species were then introduced. A fixed concentration of Lys (200 ng/mL) was prepared by dissolving Lys in PBS (0.1 % v/v in PBS, pH 7.4), and then this solution was injected into the flow-cell at a flow rate of 100 mL/h. The frequency shift corresponding to the amount of immobilized Lys was recorded.

Finally, to determine the effect of the Lys concentration on the amount of immobilized Lys, we exposed the 60 s modified ES/GA-QCM samples to varying concentrations of Lys (1–1000 ng/mL), and recorded their frequency shifts using the batch and continuous processes, as explained above.

2.6. Statistical analysis

To calculate the uniformity and nanofiber diameters in the membranes, statistical analyses were conducted using the SPSS 22.0 software for Windows. The significance was tested using

a one-way ANOVA (analysis of variance) and Tukey's HSD (honest significant difference) test. The sample size was 50 per group. The diameters are shown as the mean ± SD % and a $p < 0.05$ indicated a significant difference.

All experiments measuring frequency were independently performed 10 times, and the results are presented as the mean ± SD (standard deviation), per group. The RSD% (relative standard deviation) values for the frequency shifts were calculated by using the mean and the standard deviations, to investigate the repeatability of our frequency measurements (Ang et al., 2015).

3. Results and discussion

3.1. QCM surface modification via electrospinning

Electrospinning was used for the modification of gold electrode surfaces. Initially, we aimed to produce fine diameter (<200 nm) nanofibers to improve the protein immobilization capacity obtained through the increase in the surface-area-to-volume ratio. While operating the system, the production of a stable Taylor cone was very important; hence, the system parameters were optimized to mimic those of our previous study (Kabay et al., 2016). The optimization of working parameters was done at a constant distance of 10 cm. Our results demonstrated that when low voltages (<12 kV) were applied to the system, the Taylor cone could not be formed. At higher voltages (>21 kV), the jet became thinner, resulting in ruptures during fibre formation, which affected homogeneity. Moreover, higher flow rates resulted in uniform but thicker fibres (658±26 nm), whereas decreasing the flow rate resulted in thinner nanofibers, with an average diameter of 192±13 nm at 0.3 mL/h. For flow rates <0.3 mL/h, the Taylor cone could not be formed. While feeding the system with a 0.3 mL/h flow rate at a constant distance, the finest nanofibers could be produced at 18 kV. Accordingly, after optimizing the system parameters, the most uniform and finest nanofiber structures were obtained at an applied bias of 18 kV, a flow rate of 0.3 mL/h, and a 10 cm tip to collector distance. The diameters of 50 nanofibers were measured for the membrane, which was produced by employing optimized conditions, and their average diameter was calculated as 188±55 nm. SEM images of nanofibers used to modify ES-QCM surfaces (Fig 2. A) and their diameter distribution, including error bars (Fig 2. B), are shown in Fig.2.

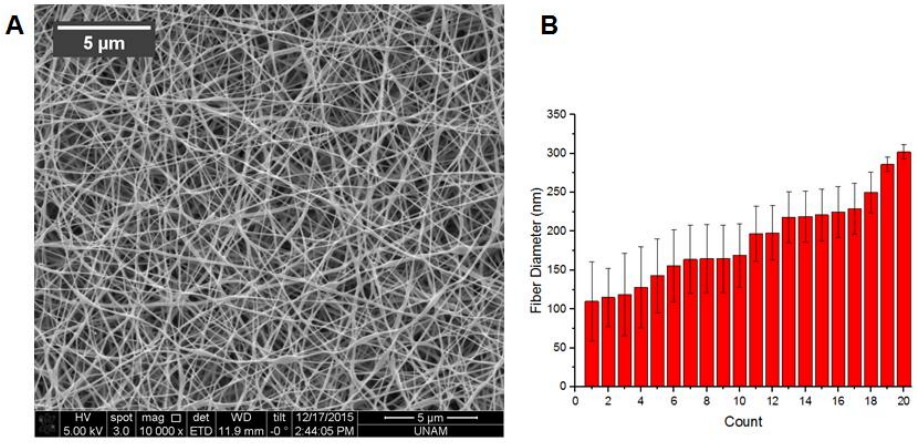

Fig. 2. SEM image of ES-BSA nanofibres collected on QCM gold electrode surface (A) and diameter distributions of nanofibres including error bars (B). Electrospinning parameters, nanofiber collection time, voltage, flow rate and tip to collector distance were: 120 s, 18 kV, 0.3 mL/h and 10 cm, respectively.

3.2. Glutaraldehyde Activation

We investigated the effect of the GA cross-linking period on nanofiber morphology and on its protein immobilization capacity. To achieve this, ES-QCM samples were cross-linked for 1–24 h. The modification of the membranes using nanofibers caused an increase in the surface area to volume ratio of the electrode surfaces, that resulted in a higher immobilization capacity. Therefore, the maintenance of a nanofibrous structure was crucial for the modification of QCM electrodes (Kabay et al., 2016; Rodoplu et al., 2013). SEM images were investigated before and after cross-linking. As clearly observed in Fig. 3, when GA was applied for less than 2 h (Fig. 3.B-C), no significant change in nanofiber morphology and no frequency shift were observed compared to non-activated nanofibrous membrane (Fig. 3.A). However, the nanofibrous structure was immediately changed into a dense membrane structure and flattened nanofibers were observed after 4 hours of cross-linking in an aqueous system (Fig. 3.E-F) (Betancor et al., 2006; Rho et al., 2006). This may be due to an insufficient period of cross-linking, due to the slow reaction kinetics between the aldehyde and amine groups (Marden et al., 2002). As a result, a 2 h cross-linking time was determined as optimal for the activation of ES-QCM surfaces. ES/GA-QCM modified nanofibrous membranes, before and after cross-linking, are shown in Fig. 3.A-F.

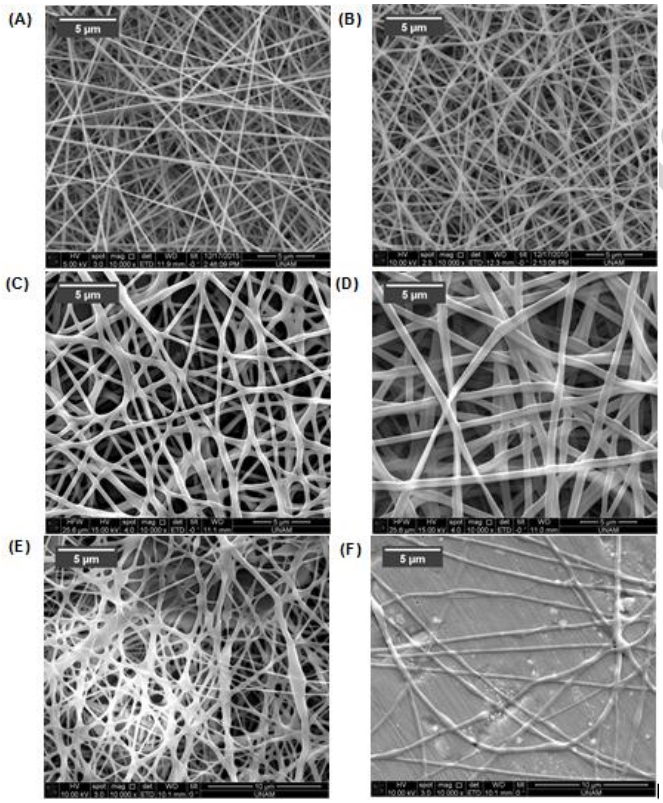

Fig. 3. E-SEM images of ES/GA-QCM samples. The images represent before (A) and after cross-linking of membranes for 0.5h (B), 1h (C), 2h (D), 4h (E) and 8h (F). Electrospinning parameters; collection time, voltage, flow rate and tip to collector distance were: 60 s, 18 kV, 0.3 mL/h and 10 cm, respectively. All other system parameters were kept constant.

3.3. Contact angle measurements

Protein adsorption is directly correlated with the surface properties and the driving forces arising from electrostatic, hydrophobic, and hydrogen-bonding interactions (Roach et al., 2005). In ultra-sensitive biosensor applications, the occurrence of adsorption is undesirable for the immobilization process. Generally, hydrophobic surfaces are considered more protein-adsorbent than hydrophilic surfaces. To avoid undesirable interactions, the surface should be hydrophilic (Israelachvili and Wennerström, 1996; Noh and Vogler, 2006; Ostuni et al., 2001).

CA measurements were performed for B-QCM, ES-QCM, and ES/GA-QCM electrodes. The results indicated that the average CA value for B-QCM electrodes was 55.3±2.8°. However, due to the amyloid-like structure, the average CA was sharply increased to 77.2±4.6° (indicative of a hydrophobic surface) for ES-QCM samples. In contrast, GA activation on hydrophobic amyloid-like protein structures resulted in a hydrophilic surface with a CA of 41.3±5.2°.

The aim of GA activation was to decrease undesired protein adsorption, while increasing the covalent interactions between the membrane surface and the model bioactive agent (Lys). As indicated above, hydrophilicity increased after GA activation.

3.3. ATR-FTIR measurements

The modified electrode surfaces were investigated using ATR-FTIR (Fig. 4). As observed from the spectra, ES-QCM showed a peak around 3300 cm^{-1} that indicated the existence of primary amine groups and hydroxyl groups in the ES-QCM membrane. Amide II groups or the −CN bending in amidine groups showed strong peaks at 1655 cm^{-1}, while another peak at 1548 cm^{-1} indicated the bending vibration of the −NH in the primary amine.

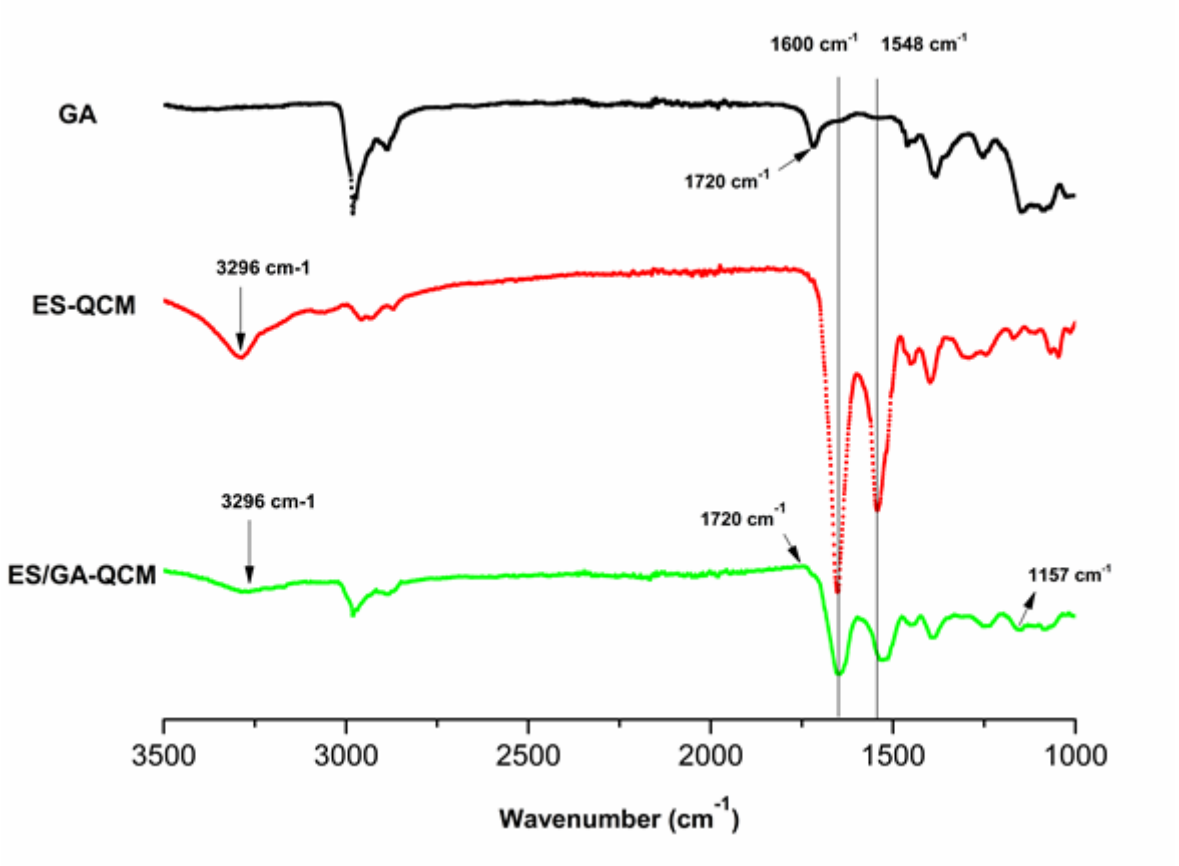

Fig. 4. ATR- FTIR spectra of pure GA, ES-QCM and ES/GA-QCM modified surfaces.

Following GA activation, the intensity of the specific peak at 3296 cm^{-1} was relatively decreased, due to the consumption of the primary amine groups and the hydroxyl groups needed for the attachment to aldehyde groups. Moreover, a new peak was observed at 1157 cm^{-1}, which corresponded to the formation of the acetal (C-O-H) group. The C=O stretch peak is the most characteristic peak for aldehyde formation. When we compared the ATR-FTIR spectrum of pure glutaraldehyde and the 2 h glutaraldehyde-activated AL-BSA nanofiber, the intensity of the aldehyde peak of the AL-BSA nanofiber at 1720 cm^{-1} was lower because of the limited exposure time (Migneault et al., 2004, Zhu and Sun, 2012).

3.4. Frequency measurements

Initial frequency measurements were carried out by employing a constant Lys concentration of 200 ng/mL. Frequency shifts caused by surface treatments applied to the B-QCMs and ES/GA-QCMs after lysozyme binding, under batch and continuous operation conditions, are given in Table 1.

Table. 1. The effect of nanofiber collection time and process type on the frequency shifts of modified QCM surfaces after Lys immobilization*.

Fibre collection period / **Type of the process**	NC	30 s	60 s	120 s
		Frequency Shifts (Hz)		
Batch (Dip and Dry)	22±12	422±128	1287±176	1434±343
Continuous (Flow-cell)	17±9	79±7	149±21	158±76

* Experimental data given as an average data from 10 crystals of replicate experiments

The average frequency of the B-QCM samples was measured as a negative control (NC) in the gas phase and calculated as 5000228±748 Hz. The small shift in the fundamental frequency (5 MHz) can be explained by the ablation that occurred during the harsh QCM cleaning process. After modifying the surfaces via electrospinning, the resonance frequency of the QCMs was measured in the gas phase. The frequency was decreased by about 2204 ± 221 Hz with an RSD of 9.98 %, which is acceptable for analytical precision, as seen for other QCM surface modifications (Alonso-Lomillo et al., 2010; Huang et al., 2014).
After measuring ES-QCM frequencies, we investigated the effect of the number of nanofibers on the immobilization capacity of the model protein (Lys), the repeatability and sensitivity of the assay. As shown in Table 1, the negative control showed a nonsignificant decrease in frequency, at 22±12 and 17±9 Hz, for batch and continuous processes, respectively. This might be caused by the physical adsorption of Lys on the ES/GA-QCM surfaces. Further, rinsing with PBS readily removed all protein molecules from the NC samples, as after this cleaning no frequency shift was observed. RSD values were found as 55 % and 52 %, for batch and continuous processes, respectively. This also showed that for the GA modified B-QCM's the repeatability was poor, because of the high deviation in frequency shifts.

For the dip-and-dry method, the frequency shifts were measured as 422±128, 1287±176, and 1434±343 Hz for the 30, 60, and 120 s collected ES/GA-QCM nanofiber samples, respectively. Our results showed that decreasing the nanofiber amounts limited both the cross-linking and the immobilization of Lys, as can be observed from the frequency shift in the 30 s modified samples, that displayed a relative standard deviation of 30.3 %. Although the highest frequency decrement was observed for the 120 s modified ES/GA-QCM sample, an overloading of the crystals caused unstable frequency shifts, which resulted in a relatively higher RSD (23 %), as compared to that in the 60 s (13.6 %) modified samples. As a result, the 60 s modified ES/GA-QCM sample showed a slightly lower frequency shift than that in the 120 s collected sample, but showed better repeatability.

In the second step, the continuous method was employed for ES/GA-QCMs. Frequency shifts were measured as 80±7, 149±21, and 157±76 Hz for the ES/GA-QCMs nanofibers collected at 30, 60, and 120 s, respectively. RSD values were measured as 9.0 %, 14.3 %, and 48.0 % (for the 30, 60, and 120 s samples, respectively). Although the highest frequency shift was observed for the ES/GA-QCM sample collected at 120 s, the repeatability was too low compared to the repeatability of the other samples (30 or 60 s) and had an RSD of 48 %. This was due to the overloading of the crystal by the solution flow and to the high content in

nanofibers. In contrast, the highest repeatability was achieved for the ES/GA-QCMs membrane at 30 s, but the frequency sensitivity for the immobilization of Lys was far lower than that in the other samples. In comparison, the ES/GA-QCM modified membranes collected at 60 s showed both an optimal frequency shift and repeatability. Therefore, these conditions were selected to investigate the protein immobilization capacity in further experiments.

Our results demonstrated that the overloading of the QCM crystal caused a decrease in the resonance frequency in both methods and in all modified ES/GA-QCM samples. When comparing the results in terms of sensitivity, the dip-and-dry method was considerably more sensitive than the flow-cell method, because of the higher reduction in frequency against the same concentration of Lys (200 ng/mL).
Lastly, the dip-and-dry and the flow-cell methods using varying concentrations of Lys were employed to determine the immobilization capacity of the 60 s modified ES/GA-QCM samples. When saturation occurs, no active spot is left on the membrane where Lys may be immobilized, due to steric hindrance and kinetic limitations (Mutlu and Mutlu, 1991; Tang et al., 2011).

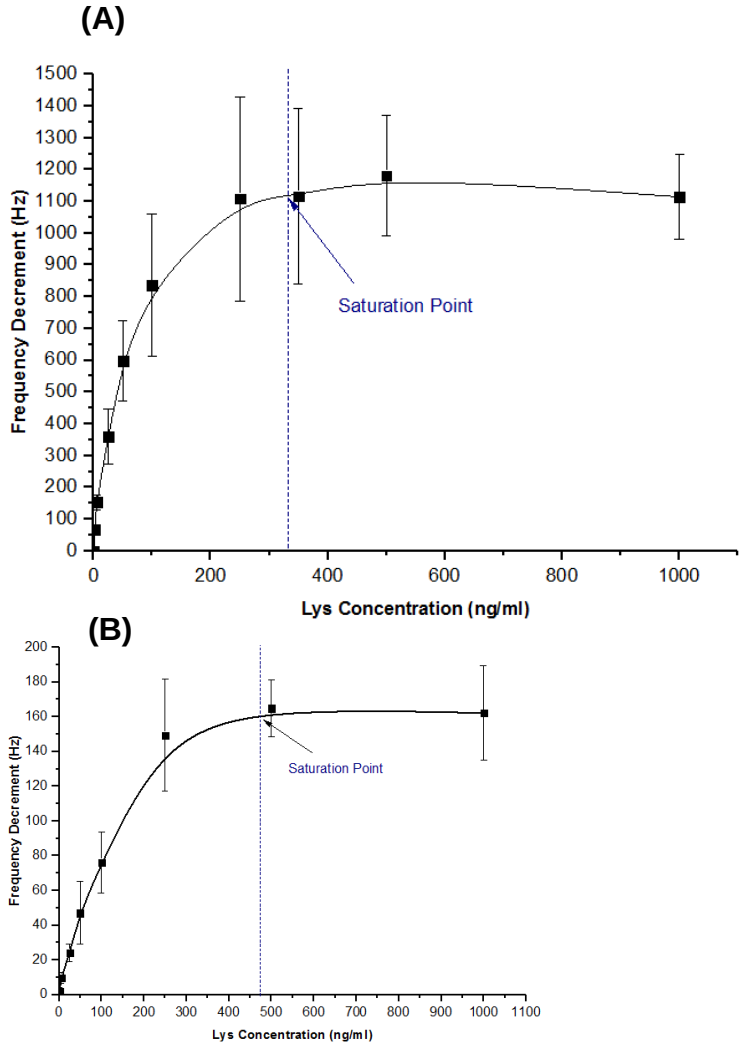

Fig. 5. Frequency shifts of modified ES/GA-QCM samples after Lys immobilization by batch (A) and continuous processes (B).

As shown in Fig. 5, our results indicated that a higher reduction in frequency, and thus a higher sensitivity, was achieved in the batch process (Fig. 5.A), compared to the continuous process (Fig. 5.B), during Lys immobilization. In the batch process, the 60 s modified ES/GA-QCM protein immobilization platform showed a linear binding trend for concentrations from 1–100 ng/mL of Lys (R^2=0.99). The highest immobilization was achieved at a Lys concentration of 335 ng/mL, and the system reached a plateau at 1112±273 Hz, due to the accumulation of Lys. In the continuous process, frequency shifts showed that the 60 s modified ES/GA-QCM platform displayed a lower sensitivity, but a wider linear binding capacity up to a Lys concentration of 250 ng/mL (R^2=0.98). The highest immobilization was achieved at a Lys concentration of 475 ng/mL, and a corresponding frequency shift was found at 149±32 Hz. The system reached a plateau at a frequency shift of 164±16 Hz, due to Lys accumulation. The RSD% values for all measurements were over 10 %.
As a result, the frequency response corresponding to the same amount of Lys was higher in the batch process than in the continuous process. This might be explained by quantitative and kinetic differences in the immobilization of Lys. Due to slow reaction kinetics between amino and aldehyde groups, the batch process facilitates the binding of proteins through a longer interaction. Moreover, the overloading of proteins on the QCM surface may lead to a reduction in sensitivity.

4. Conclusion

In conclusion, we propose a new strategy for simplifying the immobilization of bioactive molecules over a mass-sensitive transducer, by employing an infrastructure sensing layer, in the form of AL-BSA nanofibers, on QCM surfaces. Thus, we completely eliminate synthetic or polymeric methods, and the surfaces consist of a fully natural ultrathin material, containing self-functional amino groups. For electrospinning, we propose an 18-kV applied bias, a 0.3 mL/h flow rate, and a 10 cm tip-to-collector distance as optimal values. By excluding the additional chemical functionalization step, the GA activated ES/GA-QCMs allowed us to measure the frequency responses caused by the immobilization of the model Lys protein, using batch and continuous processes, with good sensitivity and reproducibility. For the immobilization of Lys, the highest frequency shifts and lowest RSD were measured as 1287.0±176.2 Hz and 13.6 % for the 60 s collected ES/GA-QCMs nanofibers. Our frequency measurements showed that the binding efficiency is almost 10-fold higher in the batch method compared to continuous process for all exposure times, due to the slow reaction kinetics between the aldehyde and amino groups. The present surface preparation strategy can be used to improve the performance of any type of immunosensor, since biologically active agents can bind a natural matrix, and the wet-chemistry step for immobilization is avoided. Furthermore, the immobilization of biologically active agents, such as antibodies, for improving mass-sensitive immunosensors is already under investigation in our research group.

Acknowledgements
This study was partially supported by the Scientific and Technological Research Council of Turkey (Project Number: 215Z047). The authors thank Dr. Nicholas Paul of Heidelberg University, Germany, and Dr. Baris Ragip Mutlu of Harvard University, Medical School, USA, for checking the scientific English terminology.

References

Akdoğan, E., Çökeliler, D., Marcinauskas, L., Valatkevicius, P., Valincius, V., Mutlu, M., 2006.Surface and Coatings Technology. 201(6), 2540-2546.

Alonso-Lomillo, M. A., Domínguez-Renedo, O., Matos, P., Arcos-Martínez, M. J., 2010. Analytica chimica acta. 665(1), 26-31.

Alp, B., Mutlu, S., Mutlu, M., 2000. Food research international. 33(2), 107-112.

Ang, L. F., Por, L. Y., Yam, M. F., 2015. PloS one. 10(3), e0111859.

Ayad, M.M., Salahuddin, N.A., Minisy, I.M., Amer, W.A., 2014. Sensors and Actuators B: Chemical. 202, 144-153.

Bard, A.J., Inzelt, G., Scholz, F., 2008. Electrochemical dictionary. Springer Science & Business Media.

Betancor, L., López-Gallego, F., Hidalgo, A., Alonso-Morales, N., Mateo, G.D.-O.C., Fernández-Lafuente, R., Guisán, J.M., 2006. Enzyme and microbial technology. 39(4), 877-882.

Cinar, G., Ceylan, H., Urel, M., Erkal, T.S., Deniz T.E., Tekinay, A.B., Dâna, A., Guler, M.O., 2012. Biomacromolecules. 13(10), 3377-3387.

Wang D., Chen G., Wang H., Tang W., Pan W., Li N., Liu F., 2013. Biosensors and Bioelectronics. 48 276–280.

Dincel, Ö., Mutlu, M., 2015. Journal of Biotechnology. (208), pp.16-17.

Dror, Y., Ziv, T., Makarov, V., Wolf, H., Admon, A., Zussman, E., 2008. Biomacromolecules. 9(10), 2749-2754.

Ferreira, G.N., Da Silva, A.C., Tomé, B., 2009. Trends in biotechnology. 27(12), 689-697.

Huang, X., Xu, J., Ji, H.F., Li, G., Chen, H., 2014. Analytical Methods. 6(13), 4530-4536.

Israelachvili, J., Wennerström, H., 1996. Nature. 379(6562), 219.

Jenik, M., Seifner, A., Lieberzeit, P., Dickert, F.L., 2009. Analytical and bioanalytical chemistry. 394(2), 523-528.

Kabay, G., Kaleli, G., Sultanova, Z., Ölmez, T.T., Şeker, U.Ö.Ş., Mutlu, M., 2016. Reactive and Functional Polymers. 103, 26-32.

Karamollaoğlu, I., Öktem H.A., and Mutlu M., 2009. Biochemical Engineering Journal. 44(2-3):142-50.

Kern, W., 1993. Handbook of semiconductor wafer cleaning technology. New Jersey: Noyes Publication, 111-196.

Khadka, D.B., Haynie, D.T., 2012. Nanomedicine: Nanotechnology, Biology and Medicine. 8(8), 1242-1262.

Koshets, I., Kazantseva, Z., Shirshov, Y.M., 2003. Semiconductor physics quantum electronics and optoelectronics. 6(4), 505-507.

Kowalczyk, T., Nowicka, A., Elbaum, D., Kowalewski, T.A., 2008. Biomacromolecules. 9(7), 2087-2090.

Lu, C., Czanderna, A.W., 2012. Applications of piezoelectric quartz crystal microbalances. Elsevier.

Marden, M.C., Cabanes-Macheteau, M., Babes, A., Kiger, L., Griffon, N., Poyart, C., Boyiri, T., Safo, M.K., Abraham, D.J., 2002. Protein science. 11(6), 1376-1383.

Migneault, I., Dartiguenave, C., Bertrand, M.J., Waldron, K.C., 2004. Biotechniques. 37(5), 790-806.

Mutlu M, Mutlu S., Rosenberg M.F., Kane J., Jones M.N., Vadgama P., 1991. J. of Materials Chemistry. 1(3), 447-450.

Mutlu S., 2011. Mass Sensitive Biosensors: Principles and Applications in Food in: Mutlu M. (Ed.), Biosensors in Food Processing, Safety, and Quality Control. Taylor and Francis, CRC Press, New York, pp. 71-89.

Mutlu, S., Saber R., Koçum C., Pişkin E., 1999. Analytical Letters. 32(2):317-22.

Mutlu, S., Çökeliler, D., Shard, A., Goktas, H., Ozansoy, B., Mutlu, M., 2008. Thin Solid Films. 516(6), 1249-1255.

Nakanishi K., Muguruma H., and Karube I., 1996. Analytical Chemistry. 68:1696-700.

Noh, H., Vogler, E.A., 2006. Biomaterials. 27(34), 5801-5812.

Nuansing, W., Frauchiger, D., Huth, F., Rebollo, A., Hillenbrand, R., Bittner, A.M., 2013. Faraday discussions. 166, 209-221.

O'sullivan, C., Guilbault, G., 1999. Biosensors and Bioelectronics. 14(8), 663-670.

Ostuni, E., Chapman, R.G., Holmlin, R.E., Takayama, S., Whitesides, G.M., 2001. Langmuir. 17(18), 5605-5620.

Öztürk, K., Durusoy, M., Pişkin, E., 2008. Journal of Bioactive and Compatible Polymers. 23(6), 579-593.

Park, I.S., Kim N., 1998. Biosensors and Bioelectronics. 13(10):1091-97.

Park, I.S., Kim D. K., Adanyi N., Varadi M., Kim. N., 2004. Biosensors and Bioelectronics. 19(7):667-74.

Raynes, J.K., Gerrard, J.A., 2013. Bionanotechnology: Biological self-assembly and its applications. 8.

Rho, K.S., Jeong, L., Lee, G., Seo, B.-M., Park, Y.J., Hong, S.-D., Roh, S., Cho, J.J., Park, W.H., Min, B.-M., 2006. Biomaterials. 27(8), 1452-1461.

Roach, P., Farrar, D., Perry, C.C., 2005. Journal of the American Chemical Society. 127(22), 8168-8173.

Rodoplu, D., Sen, Y., Mutlu, M., 2013. Nanoscience and Nanotechnology Letters. 5(4), 444-451.

Saber, R., Mutlu, S., Pişkin, E., 2002. Biosensors and Bioelectronics. 17(9), 727-734.

Sauerbrey, G., 1959. Zeitschrift für physic. 155(2), 206-222.

Tang, D., Li, Q., Tang, J., Su, B., Chen, G., 2011. Analytica chimica acta. 686(1), 144-149.

Tsai, W.-B., Chien, C.-Y., Thissen, H., Lai, J.-Y., 2011. Acta biomaterialia. 7(6), 2518-2525.

Xu, G., Zhang, S., Zhang, Q., Gong, L., Dai, H., Lin, Y., 2016. Sensors and Actuators B: Chemical. 222, 707-713.

Wu, Z., Yan Y., Shen G., and Yu R., 2000. Analytica Chimica Acta. 412, 29-35.

Zhang, C., Cappleman, B., Defibaugh-Chavez, M., Weinkauf, D., 2003. Journal of Polymer Science Part B: Polymer Physics. 41(18), 2109-2118.

Zhu, J., Sun, G., 2012. Reactive and Functional Polymers. 72(11), p. 839-845.

Highlights

- Amyloid-like bovine serum albumin (AL-BSA) nanofibrous membranes were used for the first time to modify QCM surfaces.
- Single-step modification of QCM surfaces was accomplished to eliminate multi-stage functionalization by self-functional protein modification, including wet chemistry and plasma processing.
- High sensitivity to mass change on surface against lysozyme was obtained.
- A real-time protein immobilization platform was built and potential immunosensor applications have been discussed.